ELSEVIER

Biophysical Chemistry 88 (2000) 137–152

Biophysical Chemistry

www.elsevier.nl/locate/bpc

Steady-state cyclic electron transfer through solubilized *Rhodobacter sphaeroides* reaction centres

Bart J. van Rotterdam[a,*], Hans V. Westerhoff[a,b], Ronald W. Visschers[b], Michael R. Jones[c], Klaas J. Hellingwerf[a], Wim Crielaard[a]

[a] *Swammerdam Institute for Life Sciences, University of Amsterdam, Biocentrum Amsterdam, Nieuwe Achtergracht 166, 1018 TV Amsterdam, The Netherlands*

[b] *Department of Molecular and Cellular Biology, Faculty of Biology, BioCentrum Amsterdam, Vrije Universiteit, 1087, de Boelelaan 1081 HV, The Netherlands*

[c] *Department of Biochemistry, School of Medical Sciences, University of Bristol, University Walk, Bristol BS8 1TD, UK*

Received 19 June 2000; received in revised form 29 August 2000; accepted 31 August 2000

Abstract

The mechanism, thermodynamics and kinetics of light-induced cyclic electron transfer have been studied in a model energy-transducing system consisting of solubilized *Rhodobacter sphaeroides* reaction center/light harvesting-1 complexes (so-called core complexes), horse heart cytochrome *c* and a ubiquinone-0/ubiquinol-0 pool. An analysis of the steady-state kinetics of cytochrome *c* reduction by ubiquinol-0, after a light-induced steady-state electron flow had been attained, showed that the rate of this reaction is primarily controlled by the one-electron oxidation of the ubiquinol-anion. Re-reduction of the light-oxidized reaction center primary donor by cytochrome *c* was measured at different reduction levels of the ubiquinone-0/ubiquinol-0 pool. These experiments involved single turnover flash excitation on top of background illumination that elicited steady-state cyclic electron transfer. At low reduction levels of the ubiquinone-0/ubiquinol-0 pool, the total cytochrome *c* concentration had a major control over the rate of reduction of the primary donor. This control was lost at higher reduction levels of the ubiquinone/ubiquinol-pool, and possible reasons for this behaviour are discussed.

Keywords: *Rhodobacter sphaeroides*; Reaction center; Electron transfer; Ubiquinone; Cytochrome *c*; Control theory

Abbreviations: BQ, benzoquinone; cyt *c*, cytochrome *c*; P, reaction center primary donor; pmf, proton motive force; Q_0, ubiquinone-0 (2,3-dimethoxy-5-methyl-parabenzoquinone); Q-pool, ubiquinone/ubiquinol pool; RC, reaction center; RCLH1, reaction center/light harvesting antenna-1 core complex; $\Delta\tilde{\mu}_{H^+}$, electrochemical gradient for protons

* Corresponding author. Present address: Department of Biochemistry, Lund University, Box 124, 221-00 Lund, Sweden. Tel.: +46-46-222-8144; fax: +46-46-222-4534.

E-mail address: bartvr@dds.nl (B.J. van Rotterdam).

0301-4622/00/$ - see front matter
PII: S0301-4622(00)00206-4

1. Introduction

During photosynthesis in purple non-sulfur bacteria such as *Rhodobacter* (*Rb.*) *sphaeroides*, cyclic electron transfer through the reaction center (RC) [1–3], the quinone pool, the cytochrome (cyt) b/c_1 complex [4] and cyt c_2 is coupled to the generation of an electrochemical gradient of protons ($\Delta\tilde{\mu}_{H^+}$) across the energy-transducing membrane. When scaled by the Faraday constant, this parameter is referred to as the proton motive force (pmf). Cyclic electron transfer is driven by light-energy transduction in the RC, where excitation of a 'special pair' of bacteriochlorophylls (P) at the periplasmic side of the membrane drives the reduction, after two intermediate steps, of a bound quinone (Q_A) close to the cytoplasmic side of the membrane. Under steady-state conditions in an intact membrane, light-driven electrogenic transmembrane electron transfer is catalysed in the RC, and this electron transfer takes place in the presence of the pmf. The aim of our research is to examine the extent to which the pmf controls electron pumping in the RC during light-driven cyclic electron transfer, and to identify the molecular basis for such control.

To this end we have developed a simplified model cyclic electron transfer system consisting of *Rb. sphaeroides* RCLH1 core complexes reconstituted into electrically-sealed liposomes and supplemented with ubiquinone-0/ubiquinol-0 (Q_0/Q_0H_2) and horse heart cyt *c* [5]. RCLH1 core complexes consist of RCs together with the LH1 antenna proteins and the PufX protein. Ubiquinone-0 is 2,3-dimethoxy-5-methyl-parabenzoquinone, a water-soluble analogue of the naturally-occurring ubiquinone-10 that lacks the isoprenoid side chain. Illumination of this model system oxidizes P at the donor side of the RC and reduces Q_0 at the Q_B site at the acceptor side of the RC, generating the state $P^+Q_B^-$ After two consecutive electron transfer steps Q_0H_2 is formed that dissociates from the Q_B site. Cyclic electron transfer is completed by the reduction of P^+ by the water-soluble cyt *c*, and *direct* re-reduction of cyt *c* by Q_0H_2. This abbreviated reaction sequence (omitting the steps catalysed by the cyt b/c_1 complex in the natural system) is coupled to proton translocation across the liposomal membrane and so leads to the build-up of a pmf. Cyclic electron transfer in the absence of pmf generation can also be achieved using solubilized RCLH1 core complexes supplemented with Q_0/Q_0H_2 and horse heart cyt *c*.

In order to study control of RC electron pumping by the pmf using this simplified model system it is essential to establish conditions under which any control will be associated with the electrogenic reactions inside the RC, and not in the non-electrogenic steps outside the RC. To do this, it is essential to understand in detail the characteristics of the two reactions responsible for the return of electrons from the Q_B site at the acceptor side of the RC to P^+ at the donor side. The reaction mechanism(s) and kinetic parameters of the reduction of oxidized cyt *c* (cyt c^{3+}) by Q_0H_2 in our experimental system have not been resolved, but results from the literature suggest two possible reaction mechanisms for this non-physiological reaction. Work on an analogous benzoquinone/benzoquinol system (BQ/BQH_2) has shown that at neutral pH the primary reductant of cyt *c* is the semiquinone anion ($BQ^{\bullet -}$), formed by reverse disproportionation of the benzoquinone and the benzoquinol followed rapidly by deprotonation of the semiquinone [7,25]:

$$BQH_2 + BQ \leftrightarrow 2BQH^{\bullet} \leftrightarrow 2BQ^{\bullet -} + 2H^+$$

$$BQ^{\bullet -} + \text{cyt } c^{3+} \leftrightarrow BQ + \text{cyt } c^{2+}$$

This reaction is autocatalytic, the rate depending on $[H^+]^{-2}$ and being proportional to the concentration of BQ. In contrast, studies of BQ/BQH_2 and a menadiol/menadione system (2-methyl-1,4-naphthoquinone) have shown that at acid pH the rate of cyt *c* reduction is governed by oxidation of the anionic-quinol (BQH^-) [6,7].

$$BQH^- + \text{cyt } c^{3+} \leftrightarrow BQH^{\bullet} + \text{cyt } c^{2+}$$

If the pH is above the pK_a for the semiquinone

formed by this reaction, it will deprotonate to form the semiquinone anion, $BQ^{\bullet -}$, which as shown above can also reduce cyt c^{3+} to cyt c^{2+}. The reduction of cyt c^{3+} by the anionic quinol depends on $[H^+]^{-1}$, and is not stimulated by BQ.

Rich and Bendall [6,7] have proposed that the mechanism involving the anionic quinol is the most relevant to biologically-important quinols such as ubiquinol and plastoquinol. One aim of the present study, therefore, is to determine which mechanism is relevant to the reduction of cyt c^{3+} by Q_0H_2 in our model system, which operates at pH 8.0.

The kinetics of reduction of P^+ by cyt c^{2+} have received substantial experimental attention. Biphasic reduction kinetics have been observed by several groups and different models explaining this behaviour have been proposed [8–17]. The fast component ($\tau \approx 1$ μs) shows first-order behaviour and represents effectively intermolecular electron transfer from bound cyt c^{2+} to P^+ [8,9,13,14,16,17]. The slow phase follows second order kinetics with parameters that show variation with pH and ionic strength, and involves a bimolecular collisional reaction between cyt c^{2+} and the RC [14–17].

The mechanisms for electron transfer from reduced quinone to cyt c^{3+} and from cyt c^{2+} to P^+ described above have largely been determined in experiments using dark equilibrated RCs and saturating single-turnover excitation flashes. Calculations of the electron transfer rates were based on the premise that there is relaxation back to the pre-flash (dark) equilibrium state. In this report, for the first time, we have examined re-reduction of P^+ after a saturating single-turnover flash in the presence of background illumination, which allows us to follow donor reduction until the steady-state flux induced by the background illumination is re-attained. The rates of P^+ reduction calculated, therefore, reflect the actual steady state kinetics of the system, and provide new data relevant to rates of P^+ reduction during light-driven cyclic electron transfer.

The newly studied reaction mechanisms, kinetics and thermodynamics of the reactions closing the light induced electron transfer cycle initiated by the RC are of much help for future analysis of its regulation under working conditions using model systems.

2. Materials and methods

2.1. Growth of Rb. sphaeroides and isolation of core complexes

Rb. sphaeroides strain RK1 [18] was grown anaerobically at low light intensity [19] and 30°C in filled 1-l bottles in a complex medium containing 3 mM potassium phosphate (pH 7.5), 86 mM NaCl, 3 mM $(NH_4)_2PO_4$, 0.4 mM $MgSO_4$, 0.14 mM $CaCl_2$, 10 mM D/L-malate, 4 μM nicotinamide, 1.5 μM thiamine chloride, 0.02 μM biotin, 3 g/l yeast extract, 0.5 g/l peptone and 5 g/l bactotryptone. Cells were harvested at an OD_{660} of approximately 3, washed twice in a buffer consisting of 50 mM potassium phosphate (pH 7.4), 50 mM KCl, 8 mM $MgCl_2$ and 10% (w/v) sucrose, resuspended in the same buffer and stored at −20°C until use. Intracytoplasmic membranes were prepared by three successive passages of thawed cells through a French pressure cell at 18 000 psi and 0°C. Cell debris was removed by low speed centrifugation (20 000 × *g* for 30 min at 4°C). Membranes were collected by ultra-centrifugation (200 000 g for 1.5 h at 4°C) and resuspended in the buffer described above to a final bacteriochlorophyll concentration of 1.5 mM. Membranes were stored on ice and used the same day for isolation.

RCLH1 core complexes were extracted from membranes by addition of 20 mM Na-desoxycholate (deoxycholate), 15 mM *n*-octyl-β-D-glucopyranoside (octylglucoside) and 20 mM EDTA, as described previously [5]. Non-solubilized material was removed by centrifugation (2 min at full speed in an Eppendorf centrifuge) and the supernatant was layered onto a 9-ml, 10–55% (w/v) continuous sucrose gradient in 20 mM sodium-deoxycholate, 15 mM octylglucoside, 50 mM potassium-Hepes, 50 mM KCl and 20 mM EDTA (pH 7.4). Gradients were centrifuged in a swing-out rotor at 210 000 g for 16 h. Pigmented bands were recovered from the gradient, analysed by absor-

bance spectroscopy, and stored in liquid nitrogen until use.

2.2. Measurement of cyt c concentration and redox changes

Changes of cyt *c* reduction levels (or concentrations) were monitored at $A_{550-540}$ in an Aminco DW2 double beam spectrophotometer (American Instrument Company, Silver Spring, MD) equipped with a magnetic stirrer using an $\varepsilon^{red-ox}_{550-540}$ of 20.4 mM^{-1} cm^{-1}. Measurements were performed at room temperature in 50 mM K-Hepes, 50 mM KCl (pH 8.0) under a constant flow of argon. Measuring light was detected using a photomultiplier, which was shielded from excitation light with a BG38 filter (Schott, Mainz, Germany). Oxidation of cyt *c* by solubilized RCLH1 core complexes was initiated by side-illumination of the cuvette with red light ($\lambda > 650$ nm). Reduction and oxidation rates were calculated from the tangent to the delta-absorbance traces at the appropriate cyt *c* concentration and/or time.

2.3. Measurement of P oxidation and reduction

The reduction level of P was monitored by measuring absorbance changes at 860 nm in a laboratory-built, single beam kinetic spectrophotometer with sub-millisecond time resolution. Background illumination was supplied by the measuring light (860 nm), which was passed through a monochromator. Excitation flashes from a Xenon flash lamp (EG&G FX272; 3 μs pulse width, approximately 22 J/flash) were guided to the cuvette via a quartz fibre-optic light guide, and care was taken to ensure that the flashes were saturating. Data were collected with a LeCroy 9360 digital oscilloscope; for each measurement 16 averages were taken with a 10-s interval to ensure full re-reduction of the sample between individual flashes.

2.4. Analytical methods and reagents

RC concentrations were calculated from the $\Delta\Delta A_{603-540}$ between diaminodurene-reduced and light-oxidized RCs, using an $\varepsilon^{red-ox}_{603-540}$ of 37.2 mM^{-1} cm^{-1} [20]. Bacteriochlorophyll content was measured at 772 nm in 7:2 (v/v) acetone/methanol extracts according to Clayton [21]. Absorption measurements were performed on a customized Aminco DW2a spectrophotometer (American Instrument Company, Silver Spring, MD).

Horse heart cyt *c* (Boehringer) was reduced using sodium dithionite and purified using a Sephadex G-25 gel-filtration column. Q_0 (Sigma) was dissolved in ethanol and kept at −20°C. To generate Q_0H_2, Q_0 was dissolved in methanol containing 1 mM EDTA and reduced using sodium-borohydride. After acidification by the addition of small amounts of hydrochloric acid and centrifugation, the supernatant was kept under nitrogen in the dark at −20°C to prevent re-oxidation. The percentage of Q_0H_2 after this procedure was close to 100%, as analysed by absorbance spectroscopy from the amount of cyt c^{3+} that could be reduced by the Q_0H_2 solution (data not shown).

3. Results and discussion

3.1. The kinetics of reduction of cyt^{3+} by Q_0H_2

To determine conditions under which the rate of reduction of cyt c^{3+} by Q_0H_2 in the model system is maximized and any possible control exerted by this step on cyclic electron transfer is minimized, the dependence of the rate of cyt c^{3+} reduction on the concentration of Q_0H_2 was examined. Continuous illumination was applied to solubilized core complexes until a steady-state level of oxidation of cyt *c* was achieved, at which point the actinic light was switched off and the time course of reduction of cyt c^{3+} was followed until a dark equilibrium state was reached. Comparison of the rate of reduction of cyt c^{3+} at any given redox state of cyt *c* (i.e. at any fixed $OD_{550-540}$), and at a fixed concentration of Q_0, showed that the rate of cyt c^{3+} reduction in-

creased with increasing initial concentrations of Q_0H_2 (Fig. 1). As shown in Fig. 2, under these conditions the rate of cyt c^{3+} reduction showed a first order dependence on the initial concentration of Q_0H_2. Fig. 2 also displays the dependence of the reaction on the proton activity, at fixed concentrations of Q_0H_2, Q_0, cyt c^{2+} and cyt c^{3+}. A linear fit of the rate proportional to $[H^+]^{-1}$ was obtained between pH 7.0 and 8.5, indicating that the reaction shows a first order dependence on the inverse of proton activity.

Fig. 3 shows an analysis of the time course of reduction of cyt c^{3+} under conditions similar to those in Fig. 1, and an initial concentration of Q_0H_2 of 25 μM. If the reaction is first order with respect to the concentration of cyt c^{3+} then a plot of $\ln\{[\text{cyt } c^{3+}]_{t+\delta t} - [\text{cyt } c^{3+}]_t\}$ (where δt is 14.5 s, two to three times the half time of the reaction) should exhibit a linear dependence on time [22]. If the reaction is second order with respect to the concentration of cyt c^{3+}, then a plot of $\{([\text{cyt } c^{3+}]_{t=0} - [\text{cyt } c^{3+}]_{t+\delta t})/([\text{cyt } c^{3+}]_t - [\text{cyt } c^{3+}]_{t+\delta t})\} - 1$ should be linear with time [22]. The analysis in Fig. 3 clearly shows that the reduction of cyt c^{3+} by Q_0H_2 was first order with respect to the concentration of cyt c^{3+}.

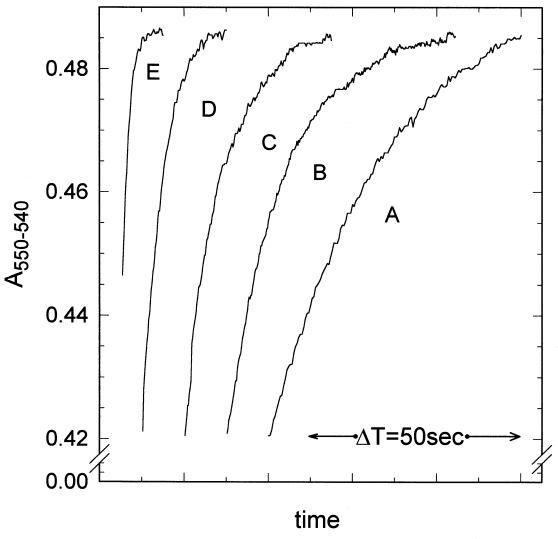

Fig. 1. Time course of reduction of cyt c^{3+} in the dark, after light-induced oxidation of cyt c^{2+} by solubilized core complexes. Conditions: [RCLH1] = 60 nM, $[Q_0]^{ini}$ = 400 μM, [cyt c^{2+}] ^{ini} = 28.7 μM, [cyt c^{3+}]^{ini} = 1.3 μM and $[Q_0H_2]^{ini}$ = 0, 25, 50, 100 and 225 μM for trace A, B, C, D and E respectively ([ ]^{ini} = initial concentration).

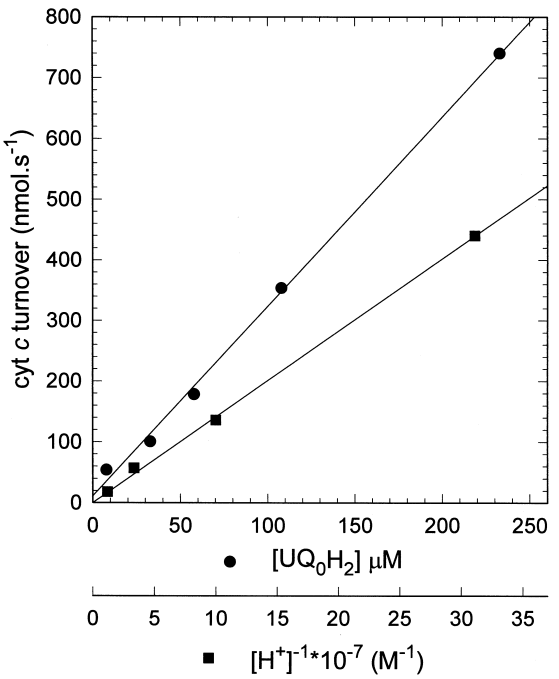

Fig. 2. Dependence of the rate of reduction of cyt c^{3+} on $[Q_0H_2]$ and the proton concentration. Circles: in the dark, after light-induced oxidation of cyt c^{2+} by solubilized core complexes, $[RCLHI]^{ini}$ = 60 nM, $[Q_0]^{ini}$ = 400 μM, [cyt c^{2+}]^{ini} = 28.7 μM, [cyt c^{3+}]^{ini} = 1.3 μM, $[Q_0H_2]^{ini}$ varied between 10 and 230 μM. Squares: With pH varying between 7.0 and 8.5, $[Q_0]$ = 150 μM, $[Q_0H_2]$ = 50 μM and [cyt c^{3+}] = 8.8 μM. The lines represent fits with a linear regression.

3.2. The mechanism of reduction of cyt c^{3+} by Q_0H_2

In any reaction that consists of two or more steps, the rate of the overall reaction can be controlled by one or more of the individual steps [23]. The location of the step that exerts the greatest control over the overall reaction is determined by the kinetic and thermodynamic properties of all the individual steps of the path-

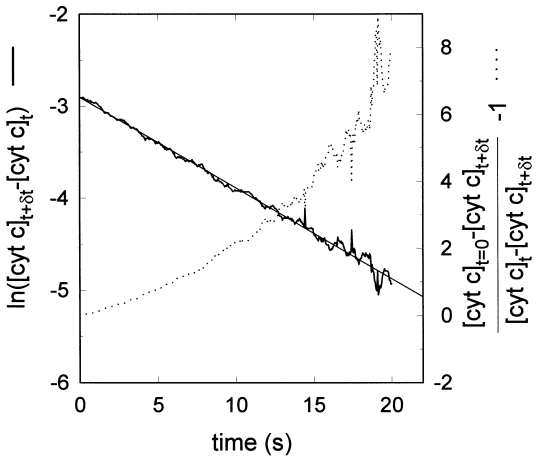

Fig. 3. Plot to determine the order of the kinetics of cyt c^{3+} reduction. The data were calculated from a time course of cyt c^{3+} reduction in the dark, after light-induced oxidation of cyt c^{2+} by solubilized core complexes. δt is two to three times the half time of the reaction. The straight line represents a fit with a linear regression. Conditions: [RCLH1] = 60 nM, $[Q_0]^{ini}$ = 400 μM, $[Q_0H_2]^{ini}$ = 25 μM, [cyt c^{2+}]^{ini} = 28.7 μM and [cyt c^{3+}]^{ini} = 1.3 μM.

way taken together. It is, therefore, important to determine the exact mechanism of reduction of cyt c^{3+} by Q_0H_2, if the distribution of control in the new experimental model system is to be understood.

The first possible reaction sequence considered is a ter-molecular reaction in which one Q_0H_2 reduces two cyt c^{3+}, similar to the mechanism proposed for the reduction of cyt c^{3+} by catechol [24]. This reaction can be written as:

$$Q_0H_2 + 2\text{cyt } c^{3+} \underset{k_{-1}}{\overset{k_1}{\leftrightarrow}} Q_0 + 2\text{cyt } c^{2+} + 2H^+$$

(Reaction 1)

According to this scheme, the rate of cyt c^{3+} reduction by Q_0H_2 exhibits a second-order dependence on the concentration of cyt c^{3+}. This is clearly inconsistent with the first order dependence found experimentally, and so this mechanism can be discounted.

In the second possible mechanism, reverse disproportionation of one molecule of Q_0H_2 and one molecule of Q_0 generates two molecules of the semiquinone $Q_0H^\bullet$. After deprotonation, the semiquinone anion, $Q_0^{\bullet-}$, reduces cyt c^{3+}. This is analogous to the mechanism proposed for a mixture of BQ and BQH_2 at neutral pH [7,25]. The scheme can be written as:

$$Q_0H_2 + Q_0 \underset{k_{-2a}}{\overset{k_{2a}}{\leftrightarrow}} 2Q_0H^\bullet \qquad \text{(Reaction 2a)}$$

$$Q_0^{\bullet-} + \text{cyt } c^{3+} \underset{k_{-2b}}{\overset{k_{2b}}{\leftrightarrow}} Q_0 + \text{cyt } c^{2+} \qquad \text{(Reaction 2b)}$$

The outcome of an analysis of this ubisemiquinone mechanism, which is given in detail in Appendix A, is also that the rate of cyt c^{3+} reduction will not exhibit a first order dependence on the concentration of cyt c^{3+}, which again is inconsistent with the experimental findings. Detailed justification of this conclusion is given in Appendix A.

A third possible reaction scheme, hereon termed the ubiquinol-anion mechanism, is that proposed for BQ/BQH_2 and menadione/menadiol at acid pH [6,7], and is shown below. In the first step, the ubiquinol-anion (Q_0H^-) reacts with cyt c^{3+} forming ubisemiquinone ($Q_0H^\bullet$). After deprotonation of the $Q_0H^\bullet$, the ubisemiquinone-anion $Q_0^{\bullet-}$ directly reduces cyt c^{3+} as in Reaction 2b, above. The overall scheme is:

$$Q_0H^- + \text{cyt } c^{3+} \underset{k_{-3a}}{\overset{k_{3a}}{\leftrightarrow}} Q_0H^\bullet + \text{cyt } c^{2+}$$

(Reaction 3a)

$$Q_0^{\bullet-} + \text{cyt } c^{3+} \underset{k_{-3b}}{\overset{k_{3b}}{\leftrightarrow}} Q_0 + \text{cyt } c^{2+} \qquad \text{(Reaction 3b)}$$

As an alternative to Reaction 3b, two $Q_0H^\bullet$ formed as shown in Reaction 3a could undergo a disproportionation reaction to yield Q_0 and Q_0H_2:

$$2Q_0H^\bullet \underset{k_{-3c}}{\overset{k_{3c}}{\leftrightarrow}} Q_0H_2 + Q_0 \qquad \text{(Reaction 3c)}$$

Including protonation/deprotonation steps, Reaction 3c is the reverse of Reaction 2a above, and regenerates Q_0H_2 for further reduction of cyt c^{3+}. Regardless of the nature of the second step when the main control of the overall reaction resides in the forward flow through Reaction 3a then, as detailed in Appendix A, the rate of cyt c^{3+} reduction by Q_0H_2 has a first order dependence on the concentrations of both cyt c^{3+} and Q_0H_2, in accord with our experimental findings. However, the analysis described in detail in Appendix A is not able to distinguish between the reaction scheme in which the semiquinone-anion is depleted through reduction of cyt c^{3+} (Reaction 3b), or where it is depleted through disproportionation (Reaction 3c). Having said this, because the concentration of cyt c^{3+} is much higher than that of the ubisemiquinone, it seems likely that the first mechanism is the more realistic, and, therefore, most probably the overall reaction is composed of Reaction 3a and Reaction 3b. In addition to these considerations, the results summarized in Fig. 2 indicate that the observed rate of the reduction of cyt c^{3+} by Q_0H_2 shows a reciprocal first-order dependence on the proton activity. This provides additional support for the conclusion that the ubiquinol-anion, Q_0H^-, is the primary reductant of cyt c^{3+}. In the ubisemiquinone mechanism, shown in Reaction 2a and Reaction 2b, the rate of cyt c^{3+} reduction should be inversely proportional to the square of the proton activity [7], in contrast to the experimental findings.

The reduction of cyt c^{3+} by benzoquinol, at neutral pH, follows the semiquinone mechanism described by Reaction 2a and Reaction 2b [7,25]. In [7] it was noted that the semiquinone mechanism should be favoured by a more alkaline pH because of the increased concentration of the fully deprotonated benzoquinol. Although the pH at which our experiments were performed was only slightly alkaline (pH 8), the pK_a values for ubiquinol-0 might be some 1.5–2 units higher than those for benzoquinol, thus reducing the concentration of the dibasic form of the ubiquinol-0 by a factor of 10^3–10^4. The semiquinone-anion of benzoquinone may also have a lower standard chemical potential than ubisemiquinone-0. These factors may also help to explain why one electron reduction of cyt c^{3+} at pH 8.0 occurs via the ubiquinol anion in the case of ubiquinone-0 rather than by the semiquinone anion mechanism.

3.3. The thermodynamics of the reduction of cyt c^{3+} by Q_0H_2

The equilibrium constants for the reduction of cyt c^{3+} by Q_0H_2 via Reaction 3a ($K_{eq[3a]}$) and Reaction 3b ($K_{eq[3b]}$) were estimated by assuming that the standard midpoint potentials of the $Q_0H^-/Q_0H^\bullet$ and $Q_0^{\bullet-}/Q_0$ redox couples have similar values to those reported for ubiquinol-1 [7] (+191 mV and −240 mV, respectively). Using these values, and a standard mid-point potential of +260 mV for horse heart cyt c^{2+}/cyt c^{3+} at pH 8 [16], values of $K_{eq[3a]} = 14.8$ and $K_{eq[3b]} = 3.0 \times 10^8$ were obtained, indicating that in both cases the forward reaction is favoured. Assuming deprotonation to generate the quinol or semiquinone anion is rapid and non-limiting in Reaction 3a and Reaction 3b, the reduction of cyt c^{3+} by Q_0H_2 in the model system can be written as:

$$Q_0H_2 + \text{cyt } c^{3+} \underset{k_{-4a}}{\overset{k_{4a}}{\leftrightarrow}} Q_0H^\bullet + \text{cyt } c^{2+}$$

(Reaction 4a)

$$Q_0H^\bullet + \text{cyt } c^{3+} \underset{k_{-4b}}{\overset{k_{4b}}{\leftrightarrow}} Q_0 + \text{cyt } c^{2+}$$

(Reaction 4b)

in which the rate constants k_{4a}, k_{-4a}, k_{4b} and k_{-4b} are pH-dependent. The equilibrium constant for Reaction 4a is related to that for Reaction 3a by:

$$K_{eq[4a]} = k_{4a}/k_{-4a} = K_{eq[3a]} \times (K_{a[QH2]}/[H^+]) \quad (1)$$

where $K_{a[QH2]}$ is the acid dissociation constant for Q_0H_2. Likewise, the equilibrium constant for Reaction 4b is related to that of Reaction 3b by:

$$K_{eq[4b]} = k_{4b}/k_{-4b} = K_{eq[3b]} \times (K_{a[SQ]}/[H^+]) \quad (2)$$

where $K_{a[SQ]}$ is the acid dissociation constant of semiquinone. At pH 8, the equilibrium constants $K_{eq[3a]}$ and $K_{eq[3b]}$ estimated above, in combination with the values $pK_{a[QH2]} = 11.25$ and $pK_{a[SQ]} = 5.9$, yielded equilibrium constants of 8.3×10^{-3} and 3.8×10^{10} for Reaction 4a and Reaction 4b, respectively. The equilibrium constant $K_{eq[1]}$ for the overall process summarized in Reaction 1, described above, equals the product of the equilibrium constants of Reaction 4a and Reaction 4b:

$$K_{eq[1]} = K_{eq[4a]} \times K_{eq[4b]} = \frac{[Q_0]_{eq}[\text{cyt } c^{2+}]^2_{eq}}{[Q_0H_2]_{eq}[\text{cyt } c^{3+}]^2_{eq}} \quad (3)$$

The value of $K_{eq[1]}$ was 3.2×10^8, heavily favouring the overall forward reaction.

3.4. The kinetics of reduction of cyt c^{3+} by Q_0H_2

In our experiments, the rate of the overall process summarized in Reaction 1 was measured. The rate (v) of this reaction can be expressed in terms of the rate constants for Reaction 4a (v_{4a}) and Reaction 4b (v_{4b}). In a steady-state condition, v_{4a} will equal v_{4b}, and as $d[Q_0H^\bullet]/dt$ will equal zero at steady-state, then the rate of the overall reaction is given by:

$$v = \frac{\left\{ \begin{array}{l} k_{4a}k_{4b}[Q_0H_2][\text{cyt } c^{3+}]^2 \\ \quad -[k_{-4a}k_{-4b}[Q_0][\text{cyt } c^{2+}]^2 \end{array} \right\}}{k_{-4a}[\text{cyt } c^{2+}] + k_{4b}[\text{cyt } c^{3+}]} \quad (4)$$

As cyt c^{3+} is reduced in both steps of the overall reaction, the rate of cyt c^{3+} reduction is given by:

$$-d[\text{cyt } c^{3+}]/dt = v_{4a} + v_{4b} = 2v \quad (5)$$

and with the following definitions for the apparent rate constants:

$$k^{\#}_{4a} = \frac{k_{-4a}}{K_{eq[4a]}} \times \frac{k_{4b}[\text{cyt } c^{3+}]}{k_{4b}[\text{cyt } c^{3+}] + k_{-4a}[\text{cyt } c^{2+}]} \quad (6)$$

and:

$$k^{\#}_{-4b} = \frac{k_{4b}}{K_{eq[4b]}} \times \frac{k_{-4a}[\text{cyt } c^{2+}]}{k_{4b}[\text{cyt } c^{3+}] + k_{-4a}[\text{cyt } c^{2+}]} \quad (7)$$

the rate equation [Eq. (4)] can be written as a function of the apparent rate constants $k^{\#}_{4a}$ and $k^{\#}_{4b}$ in the following way:

$$v = -\frac{d[\text{cyt } c^{3+}]}{2dt} = k^{\#}_{4a}[Q_0H_2][\text{cyt } c^{3+}] - k^{\#}_{4b}[Q_0][\text{cyt } c^{2+}] \quad (8)$$

It should be noted that the cyt c concentration terms occur linearly in this equation, the forward and reverse rates referring to different steps in the reaction sequence. The magnitude of $k^{\#}_{4a}$ was determined from experiment to be 8.2×10^2 M^{-1} s^{-1} (see Table 1), and by use of the equilibrium concentrations and Eq. (8), the rate constant $k^{\#}_{-4b}$ was calculated. Its value depended on the reduction state of cyt c. We conclude that Eq. (8), with these rate constants, is sufficient to describe the reduction of cyt c^{3+} by Q_0H_2. This will allow us to express the rate of the overall reaction as a function of spectroscopically measurable concentrations.

Because the reaction is first order in [cyt c^{3+}], the elasticity coefficient of the overall rate vs. the concentration of cyt c^{3+} must equal 1:

Table 1
Values for the rate constants (k_{4a} and k_{-4a}) and redox potential difference (ΔE^0) of the reaction between $Q_0H_2/Q_0H^\bullet$ and cyt c^{3+}/cyt c^{2+} at pH 8.0[a]

	Rate constant	S.E.M. ($n = 20$)
	(M^{-1} s^{-1})	
$k_{4a}{}^{\#}$ and k_{4a}	8.2×10^{2}[b]	1.1×10^{2}
k_{-4a}	10.3×10^{4}[c]	

[a]The value of the apparent rate constant for the forward reaction ($k_{4a}^{\#}$) was determined from the initial rate of cyt c^{3+} re-reduction after a steady state light-induced level of cyt c oxidation was reached.
[b]Values obtained from experiment.
[c]Calculated values (see text). *Abbreviation:* S.E.M., standard error of the mean.

$$\varepsilon^{v}_{[\text{cyt } c^{3+}]} = \frac{\delta \ln v_{[4]}}{\delta \ln[\text{cyt } c^{3+}]} = 1 \tag{9}$$

The solution of this differential equation is only valid when:

$$k_{4b}[\text{cyt } c^{3+}] \gg k_{-4a}[\text{cyt } c^{2+}] \tag{10}$$

and:

$$[\text{cyt } c^{3+}] \gg [\text{cyt } c^{2+}]\sqrt{\frac{[Q_0]}{3 \times 10^{8}[Q_0H_2]}} \tag{11}$$

Using Eq. (10), Eq. (6) simplifies to:

$$k_{4a}^{\#} = \frac{k_{-4a}}{K_{\text{eq}[4a]}} = k_{4a} \tag{12}$$

and Eq. (7) simplifies to:

$$k_{-4b}^{\#} = \frac{k_{-4a}[\text{cyt } c^{2+}]}{K_{\text{eq}[4b]}[\text{cyt } c^{3+}]} \tag{13}$$

Calculated from the measured $k_{4a}^{\#}$, the rate constant k_{4a} approximates to 8.2×10^{2} M^{-1} s^{-1}. Using Eq. (1), and the value for $K_{\text{eq}[4a]}$ estimated above, the rate constant k_{-4a} can then be estimated to be 10.3×10^{4} M^{-1} s^{-1} (Table 1). Because the catalytic activity of Reaction 4b is so much higher than that of Reaction 4a, the control exerted by Reaction 4b on flux through the overall Reaction 1 probably approaches zero, and hence Reaction 4b would be expected to have no control on the rate of reduction of cyt c^{3+}.

3.5. Reduction of the oxidized primary donor by cyt c^{2+}

Upon the absorption of a photon, charge separation in the RC generates the state $P^+Q_A^-$ or $P^+Q_B^-$, depending upon the occupancy of the Q_B site and the redox state of the ubiquinone bound at that site. The P^+ cation is re-reduced by cyt c^{2+}. To investigate the influence of the concentration of cyt c^{2+} and of the reduction state of the Q-pool on the rate of re-reduction of P^+, the decay of flash-induced P^+ was monitored on a millisecond timescale by measuring changes in absorbance at 860 nm, as described in Section 2. The experiments were performed at a fixed (background) steady-state level of P^+, exploiting the actinic effect of the measuring beam. Additional excitation of the sample through a short flash of light caused an instantaneous decrease in absorbance at 860 nm, demonstrating further formation of P^+. Recovery of P ground state absorbance occurred during the first few milliseconds after the flash and, for most values of [cyt c^{2+}] examined, the absorbance returned to close to the pre-flash level with a half-time of 10 ms or less (Fig. 4). In the presence of either an oxidized Q-pool (Fig. 4A), or a 50% reduced Q-pool (Fig. 4B), the rate of P^+ reduction increased with increasing [cyt c^{2+}]. However, the rate of P^+ reduction became saturated at lower [cyt c^{2+}] in the presence of a 50% reduced Q-pool than in the presence of a fully oxidized Q-pool (Fig. 4B compared with Fig. 4A). Also, at equivalent, subsaturating concentrations of added cyt c^{2+}, the rate of P^+ reduction was slower in the presence of a 50% reduced Q-pool than in the presence of a fully oxidized Q-pool. This can be seen, for example, by comparing trace b in Fig. 4B with trace a in Fig. 4A.

At both tested reduction states of the Q-pool, an additional slow phase of P^+ reduction was

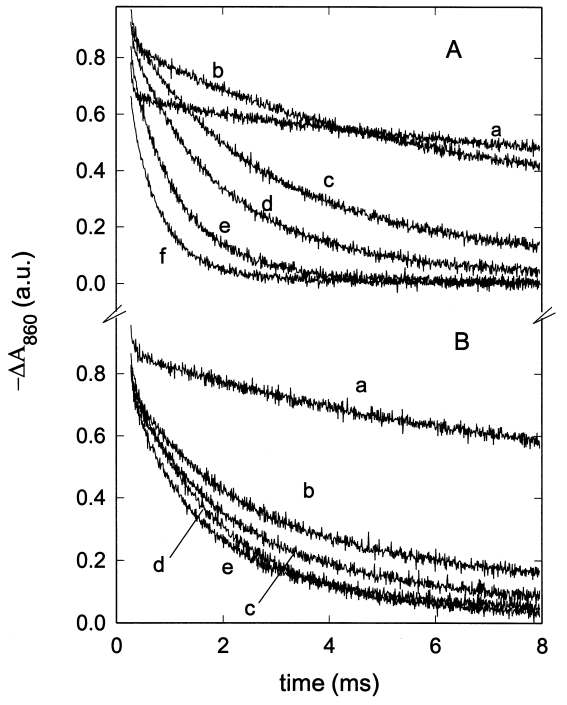

Fig. 4. Reduction of P^+ in solubilized core complexes as a function of the concentration of cyt c^{2+} and the reduction state of the Q-pool. The reduction of P^+ was measured at 860 nm after a saturating single turnover flash, delivered on top of background illumination which induced a steady state oxidation level of P. Transients were recorded under conditions of (A) [RCLH1] = 300 nM, $[Q_0]^{ini} = 400$ μM, $[Q_0H_2]^{ini} = 0$ μM and [cyt c^{2+}] = 9.2 μM (a); 17.9 μM (b); 26.3 μM (c); 34.1 μM (d); 58.6 μM (e); 127.3 μM (f). (B) [RCLH1] = 300nM, $[Q_0]^{ini} = 200$ μM, $[Q_0H_2]^{ini} = 200$ μM and [cyt c^{2+}] = 4.7 μM (a); 9.4 μM (b); 13.6 μM (c); 22.4 μM (d); μM (e). Parameters obtained from fits of the traces are given in Tables 2 and 3 for (A) and (B), respectively.

observed when [cyt c^{2+}] was low. Deconvolution of the traces obtained with the fully oxidized Q-pool (Fig. 4A) confirmed the presence of this slow phase ($\tau > 8$ ms) which, on the millisecond time-scale of the traces in Fig. 4, was fitted as an offset. In the presence of a fully oxidized Q-pool, deconvolution revealed in addition to this slow phase of P^+ decay a mono-exponential fast phase, the rate of which was dependent upon [cyt c^{2+}]. The parameters of the fits to the traces in Fig. 4A are given in Table 2. As indicated above, the lifetime of this fast phase decreased linearly with increasing [cyt c^{2+}], as shown in Fig. 5.

The kinetics of P^+ reduction measured in the presence of a 50% reduced Q-pool (Fig. 4B) were best fit by a bi-exponential decay together with the minor, slow component ($\tau > 8$ ms) described above, which was fitted as an offset. The parameters of the fits to the traces in Fig. 4B are shown in Table 3. The first exponential component, the lifetime of which was dependent on [cyt c^{2+}], was assumed to have the same origin as the exponential component fitted to the decay of P^+ in the presence of a fully-oxidized Q-pool. The lifetime of this component was therefore calculated from the data shown in Fig. 5 for P^+ decay in the presence of an oxidized Q-pool, and fixed within the fit to the data shown in Fig. 4B. The second exponential component was faster than the first, was independent of the [cyt c^{2+}] (Table 3), and was fitted as a variable component.

3.6. Mechanism of reduction of P^+ by cyt c^{2+} in the presence of a fully oxidized Q-pool

Fig. 5 shows the dependence of the lifetime of the fast component of P^+ reduction in the presence of an oxidized Q-pool, on [cyt c^{2+}]. As at all values [cyt c^{2+}] was much greater than [P^+], much of the second-order behaviour of the reaction was lost, and the rate of reduction of P^+ gave the appearance of being first order with respect to [cyt c^{2+}]. The second-order rate constant for this re-reduction, k_{CP}, was calculated to be 1.2×10^7 M^{-1} s^{-1}. The relative amplitude of the [cyt c^{2+}]-independent slow phase of P^+ reduction (the offset parameter in Table 2) decreased progressively with increasing [cyt c^{2+}], and contributed less than 10% of the overall decay at [cyt c^{2+}] > 25 μM. A possible origin of this slow phase is a fraction of P^+ that is not reduced by cyt c^{2+}, but instead decays via the charge recombination reactions $P^+Q_A^- \rightarrow PQ_A$ and/or $P^+Q_B^- \rightarrow PQ_B$. In accord with this, both the relative and absolute amplitude of the slow phase increased with decreasing [cyt c^{2+}] (Table 2) which would be the expected behaviour for a reaction competing with re-reduction of P^+ by cyt c^{2+}. Evidence in favour of this proposal was

Table 2
Parameters from fits of the transients in Fig. 4A, showing P^+ reduction by cyt c^{2+} in the presence of an oxidized Q-pool[a]

[cyt c^{2+}] (μM)	τ (ms)	Amp.	Offset	Offset/(offset + amp.) (%)
9.7	6.88	0.016	0.0242	60.2
17.9	5.25	0.034	0.0179	34.5
26.3	2.55	0.052	0.0063	10.8
34.1	1.75	0.056	0.0027	4.6
58.6	0.98	0.059	0.0007	1.2
127.3	0.65	0.053	0.0005	0.9

[a]Conditions as for legend to Fig. 4A. Each transient was fitted with a single exponential function and an offset. *Abbreviation:* Amp., amplitude.

sought by determining the rate of reduction of P^+ in the absence of cyt c^{2+}. The results of these measurements are presented in Fig. 6A. The observed first order rate constant for the charge recombination reaction (k_{CR}^{obs}), in the presence of a fully oxidized Q-pool was 1.3 s^{-1}, indicating that the reaction primarily involved charge recombination from Q_B [26,27].

3.7. Mechanism of reduction of P^+ by cyt c^{2+} in the presence of a partially reduced Q-pool

An accurate fit of the transients obtained for reduction of P^+ by cyt c^{2+} in the presence of a 50% reduced Q-pool required two exponential components, the faster of which had a lifetime that was independent on [cyt c^{2+}] and had an average value of 1.21 ms (Table 3). Both the absolute and relative contribution of this [cyt c^{2+}]-independent phase decreased with increasing [cyt c^{2+}]. Addressing the origin of this phase, at low [cyt c^{2+}] and a high reduction level of the Q-pool (i.e. a lower net concentration of Q_0), it is feasible that the lifetime of exchange of Q_0 and Q_0H_2 at the Q_B site could exert significant control on the rate of cyt c^{3+} re-reduction, and therefore on the rate of reduction of P^+. Assuming that such control operates, and using the second exponential component of the decay of P^+ to calculate a pseudo first order rate constant for Q_0 association (k_{Qex}), a value of 2.1×10^6 M^{-1} s^{-1} is obtained (taking into account that $dP^+/dt = 2 \times dQ/dt$ due to the two electron chemistry of Q_0). Accurate fitting of the re-reduction of P^+ in the presence of a partially reduced Q-pool also required a minor, slow component analogous to that ascribed above to charge recombination in a minor fraction of RCs. Fig. 6B shows a measurement of the rate of P^+ reduction in the absence of cyt c^{2+} but in the presence of a 50% reduced Q-pool. The observed first order rate constant k_{CR}^{obs} under these conditions was 3.1 s^{-1}, more than a factor of two faster than in the presence of a fully oxidized Q-pool (see above),

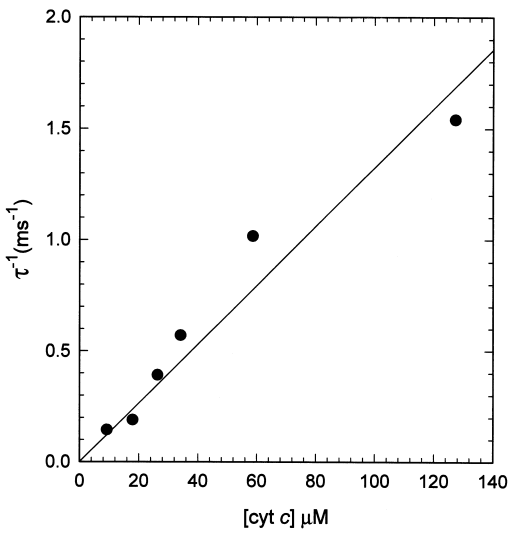

Fig. 5. The dependence of the life-time of the fast phase of P^+ reduction on the concentration of added cyt c^{2+}, with an oxidized Q-pool. Data points were calculated from the traces presented in Fig. 4A, and are given in Table 2. The solid line represents a fit with a linear regression.

Table 3
Parameters from fits of the transients in Fig. 4B, showing P^+ reduction by cyt c^{2+} in the presence of a Q-pool that was 50% reduced[a]

[cyt c^{2+}] (μM)	τ_1 (ms)	Amp. 1	τ_2 (ms)	Amp. 2	Offset	Amp. 1/(amp. 1 + amp. 2) (%)
4.7	15.7	0.012	1.50	0.050	−0.0054	19.4
9.4	7.3	0.014	1.09	0.043	−0.0020	25.1
13.6	5.0	0.023	1.29	0.024	0.0049	49.4
22.4	3.1	0.030	0.97	0.021	0.0029	58.9

[a]Conditions as for legend to Fig. 4B. Each transient was fitted with two exponential functions and an offset. *Abbreviation:* Amp. = amplitude.

which could indicate an increased contribution of the reaction $P^+Q_A^- \rightarrow PQ_A$ to charge recombination in the RC.

3.8. Control of the rate of P^+ reduction

In the analysis presented above it is apparent that the number of kinetic components required to account for reduction of P^+ in the model system varies with the reduction-state of the Q-pool, an extra component being required when the Q-pool was reduced. With an oxidized Q-pool, and in the absence of cyt c^{2+}, a slow phase of $\tau > 300$ ms accounted for most of the reduction of P^+, this corresponding to charge recombination in the RC (Fig. 6A). On titrating in cyt c^{2+}, the rate of P^+ reduction increased in the expected manner.

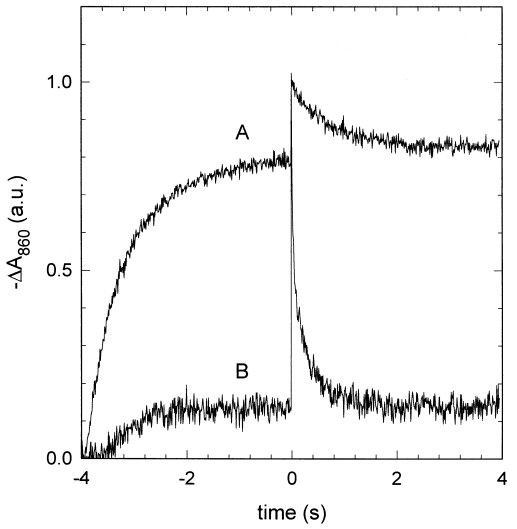

Fig. 6. Reduction of P^+ in solubilized core complexes as a function of the reduction state of the Q-pool., in the absence of cyt *c*. The reduction of P^+ was measured at 860 nm after a saturating single turnover flash, delivered on top of background illumination which induced a steady state oxidation level of P. Transients were recorded under conditions of (A) [RCLH1] = 300 nM, $[Q_0]^{ini}$ = 400 μM and $[Q_0H_2]^{ini}$ = 0 μM. (B) [RCLH1] = 300 nM, $[Q_0]^{ini}$ = 200 μM and $[Q_0H_2]^{ini}$ = 200 μM.

At low concentrations of Q_0H_2 and at significant concentrations of cyt c^{2+}, most of the control of the rate of P^+ reduction was associated with the reduction of P^+ by cyt c^{2+}, and increasing the concentration of added cyt c^{2+} caused an increase in the rate of P^+ reduction. However, when the reduction state of the Q-pool was increased, the control of the rate of P^+ reduction appeared to shift away from the cyt $c^{2+} \rightarrow P^+$ reaction, as the rate of P^+ reduction became less sensitive to increases in the concentration of added cyt c^{2+} than was the case when Q_0H_2 was absent (Fig. 4B compared with Fig. 4A). This dependence of the rate of the reaction cyt $c^{2+} \rightarrow P^+$ on the amount of Q_0H_2 is probably a consequence of the steady-state background to the experiment. It should be remembered that the background light-intensity, total concentration of the RCs, total concentration of cyt *c* and the redox state of ubiquinone are essentially fixed in the measurements carried out above. The redox state of the RC and of cyt *c* are variable, and are set by the background light during the steady-state period prior to the excitation flash. Consequently, in the experiment carried out with a 50% reduced

Q-pool (Fig. 4B), the steady-state reduction level of cyt *c* prior to the flash may be much higher than in the experiment carried out with a fully oxidized Q-pool (Fig. 4A). At equivalent total concentrations of added cyt *c*, in the 5–30 μM range, the rates of P^+ reduction seen with a 50% reduced Q-pool are probably higher than those seen with a fully oxidized Q-pool because more of the cyt *c* pool is reduced and is able to reduce P^+.

In support of this proposal, we have found that at low overall cyt *c* concentrations and with an oxidized Q-pool, the steady state level of P reduction is lower, due to actinic light-induced oxidation, than with a 50% reduced Q-pool (data not shown). This will have the effect of decreasing the rate of P^+ reduction in comparison to that obtained with a with a 50% reduced Q-pool where, due to the higher amounts of Q_0H_2, the steady-state cyt *c* reduction level will remain significantly higher. At total cyt *c* concentrations above 30 μM, the amount of reduced cyt *c* appears to be sufficiently high to maintain a rate of P^+ reduction that is independent of the redox state of the Q-pool. In addition, increasing the total concentration of cyt *c* beyond 30 μM does not bring about a faster rate of P^+ reduction. A possible explanation for this is that, with a 50% reduced Q-pool and cyt *c* concentrations above 30 μM, the exchange of Q_0H_2 from the RC for a Q_0 from the Q-pool becomes limiting, and so exerts control on the rate of P^+ reduction. The rate constant that we estimated for Q binding at the Q_B site based on the above interpretations was five times smaller than the value of 1×10^7 $M^{-1}s^{-1}$ measured by Kleinfeld et al. [28], who measured the exchange rate by the RCs through monitoring the rate of cyt *c* oxidation under conditions where the exchange of Q_{10} was controlling the reaction. This suggest that the isoprenoid tail of the quinone increases the association rate to the Q_B pocket.

Values in the literature for the rate constant for P^+ reduction by cyt c^{2+} (k_{CP}) show considerable variation, as k_{CP} strongly depends on temperature, ionic strength, pH and on the cyt *c* species used [14–16]. Tiede et al. [16] found a rate constant of 1×10^9 M^{-1} s^{-1} for photo-oxidation of horse heart cyt *c*, but stated that second order rate constants were found to vary by a factor greater than 10^6. Venturoli et al. [14] found a value of 1.4×10^9 $M^{-1}s^{-1}$ for cyt c_2. Prince et al. [15] showed that by increasing the ionic strength from 10 to 360 mM, the half-time of the reaction increased by 100-fold. Extrapolation of the values given in Prince et al. [15] to the steady-state conditions used in our system results in a rate constant of the same order of magnitude as the value $k_{CP} \approx 1.2 \times 10^7$ M^{-1} s^{-1} reported above for our model cyclic electron transfer system.

4. Conclusions

To conclude, the experiments and analysis presented above for the first time clarify the reaction mechanism and rate constants for the reactions between the Q_0-pool and horse heart cyt *c*. The principal reductant of cyt c^{3+} is the ubiquinol anion, Q_0H^-, and the $Q_0H^- \rightarrow$ cyt c^{3+} reaction has the major control over the overall rate of reduction of cyt c^{3+} under our experimental conditions. Rate constants have also been determined for charge recombination in the RC and for the reaction between cyt *c* and P^+ by measuring under steady-state conditions and different redox levels of the Q_0-pool. Most importantly the experiments demonstrate that control in the model electron transfer system can be shifted to reactions which shuttle electrons from the acceptor side of the RC to the donor side, by varying the redox poise of the Q-pool and the total concentration of cyt *c*.

Using these findings, it is now possible to define conditions under which maximum control over light-driven cyclic electron transfer is associated with the bacterial RC. The identification of these conditions is a prerequisite for a study of the effects of energy storage in the proton motive force on photosynthetic electron transfer within the RC.

Appendix A: Ubisemiquinone mechanism

Mechanism 2 for the reduction of cyt c^{3+} by

Q_0H_2 involves two reactions, which after simplifying by excluding the role of protons and protonation states can be written as:

$$Q_0^{2-} + Q_0 \underset{k_{-2a}}{\overset{k_{2a}}{\leftrightarrow}} 2Q_0^{\bullet -} \qquad \text{(Reaction 2a)}$$

$$Q_0^{\bullet -} + \text{cyt } c^{3+} \underset{k_{-2b}}{\overset{k_{2b}}{\leftrightarrow}} Q_0 + \text{cyt } c^{2+} \qquad \text{(Reaction 2b)}$$

If the rate of the reverse Reaction 2b (k_{-2b}) is neglected on the basis that Reaction 2a is far from equilibrium compared with Reaction 2b, due to the high standard chemical potential of $Q_0^{\bullet -}$ [7], then the overall rate (v) of reduction of cyt c^{3+} through Reaction 2a and Reaction 2b can be described by:

$$v = \frac{\left\{ \begin{array}{c} -k_{2b}^2[\text{cyt } c^{3+}]^2 + k_{2b}[\text{cyt } c^{3+}] \\ \sqrt{k_{2b}^2[\text{cyt } c^{3+}]^2 + 8k_{-2a}\left(2k_{2a}\left[Q_0^{2-}\right][Q_0]\right.} \\ \left. + k_{-2b}[Q_0][\text{cyt } c^{2+}]\right) \end{array} \right\}}{4k_{-2a}} \qquad \text{(A1)}$$

In the case where control of the overall reaction is confined to Reaction 2a, then Eq. (A1) can be simplified to:

$$v = 2k_{2a}\left[Q_0^{2-}\right][Q_0] \qquad \text{(A2)}$$

Neither Eq. (A1) nor Eq. (A2) yields the observed first order dependence of v on the concentration of cyt c^{3+} (Fig. 3), and so mechanism 2 is inconsistent with our experimental results.

In mechanism 3, the ubiquinol-anion (Q_0H^-) reacts with cyt c^{3+}, forming ubisemiquinone ($QH^{\bullet}$). After deprotonation to form the semiquinone anion, one option is that disproportionation occurs to yield Q_0 and Q_0^{2-}. Again, ignoring protons and protonation states, this can be written as:

$$Q_0^{2-} + \text{cyt } c^{3+} \underset{k_{-3a}}{\overset{k_{3a}}{\leftrightarrow}} Q_0^{\bullet -} + \text{cyt } c^{2+} \qquad \text{(Reaction 3a)}$$

$$2Q_0^{\bullet -} \underset{k_{-3c}}{\overset{k_{3c}}{\leftrightarrow}} Q_0^{2-} + Q_0 \qquad \text{(Reaction 3c)}$$

If the possibility of control of the overall flux through Reaction 3a and 3c by the disproportionation of $Q_0^{\bullet -}$ (k_{3c}) is neglected, then the overall rate equation reads:

$$v = \frac{\left\{ \begin{array}{c} -k_{-3a}^2[\text{cyt } c^{2+}] \\ +\sqrt{k_{-3a}^2[\text{cyt } c^{2+}]^2 + 8k_{3c}(2k_{-3c}[Q_0^{2-}][Q_0]} \\ \left. +k_{3a}[Q_0^{2-}][\text{cyt } c^{3+}]\right) \end{array} \right\}^2}{16k_{3c}} \qquad \text{(A3)}$$

and if there is little control in the reverse of Reaction 3a (k_{-3a}) then Eq. (A3) becomes:

$$v = k_{3c}\left\{ \frac{k_{3a}\left[Q_0^{2-}\right][\text{cyt } c^{3+}] + 2k_{-3c}\left[Q_0^{2-}\right][Q_0]}{k_{-3c}[\text{cyt } c^{2+}]} \right\}^2 \qquad \text{(A4)}$$

which again is inconsistent with the observed first order dependency of the reaction on [cyt c^{3+}] and [Q_0^{2-}] (i.e. [Q_0H_2]). However, if the disproportionation of $Q_0^{\bullet -}$ is much more active than the re-oxidation of cyt c^{2+} (i.e. k_{-3a} approaches 0), Eq. (A3) becomes:

$$v \approx \frac{1}{2}\left(k_{3a}\left[Q_0^{2-}\right][\text{cyt } c^{3+}]\right) + k_{-3c} + k_{3c}\left[Q_0^{2-}\right][Q_0] \qquad \text{(A5)}$$

The second term in Eq. (A5) deals with the reverse disproportionation in Reaction 3c. If this term is small, then there is a first order dependency on [Q_0H_2] and [cyt c^{3+}] which is consistent with our experimental findings.

Rather than undergoing the disproportionation Reaction 3c after the formation of the semiquinone in Reaction 3a, the semiquinone may also react with cyt c^{3+} (i.e. undergo Reaction 3b):

$$Q_0^{\bullet -} + \text{cyt } c^{3+} \underset{k_{-3b}}{\overset{k_{3b}}{\leftrightarrow}} Q_0 + \text{cyt } c^{2+} \qquad \text{(Reaction 3b)}$$

in this case:

$$v = \frac{\left\{ \begin{array}{l} k_{3b}k_{3a}\left[Q_0^{2-}\right][\text{cyt } c^{3+}]^2 - \\ k_{-3b}k_{-3a}[Q_0][\text{cyt } c^{2+}]^2 \end{array} \right\}}{k_{-3a}[\text{cyt } c^{2+}] + k_{3b}[\text{cyt } c^{3+}]} \quad \text{(A6)}$$

As the reverse reaction is negligible in view of the equilibrium constant of the overall reaction, this mechanism is consistent with the finding of first order kinetics both in [cyt c^{3+}] and [Q_0^{2-}] (i.e. [Q_0H_2]) provided that: k_{3b}[cyt c^{3+}] $\gg$ k_{-3a}[cyt c^{2+}], in which case:

$$v \approx k_{3a}\left[Q_0^{2-}\right][\text{cyt } c^{3+}] \quad \text{(A7)}$$

References

[1] C. Kirmaier, D. Holten, Primary photochemistry of reaction centers from the purple bacteria, Photosynth. Res. 13 (1987) 225–260.

[2] M.Y. Okamura, G. Feher, Proton transfer in reaction centers from photosynthetic bacteria, Annu. Rev. Biochem. 61 (1992) 862–896.

[3] G. Feher, J.P. Allen, M.Y. Okamura, D.C. Rees, Structure and function of bacterial photosynthetic reaction centers, Nature 339 (1989) 111–116.

[4] R.B. Gennis, B. Barquera, B. Hacker et al., The bc1 complexes of *Rhodobacter sphaeroides* and *Rhodobacter capsulatus*, J. Bioenerg. Biomembr. 25 (1993) 195–209.

[5] D. Molenaar, W. Crielaard, K.J. Hellingwerf, Characterization of protonmotive force generation in liposomes reconstituted from phosphatidylethalonamine, reaction centers with light harvesting complexes isolated from *Rhodopseudomonas palustris*, Biochemistry 27 (1988) 2014–2023.

[6] P.R. Rich, D.S. Bendall, A mechanism for the reduction of cytochromes by quinols in solution and its relevance to biological electron transfer reactions, FEBS Lett. 105 (1979) 189–194.

[7] P.R. Rich, D.S. Bendall, The kinetics and thermodynamics of the reduction of cytochrome *c* by substituted *p*-benzoquinols in solution, Biochim. Biophys. Acta 592 (1980) 506–518.

[8] R.E. Overfield, C.A. Wraight, Oxidation of cytochromes c and c2 by bacterial photosynthetic reaction centers in phospholipid vesicles. 2. Studies with negative membranes, Biochemistry 19 (1980) 3328–3334.

[9] R.E. Overfield, C.A. Wraight, Oxidation of cytochromes c and c2 by bacterial photosynthetic reaction centers in phospholipid vesicles. 1. Studies with neutral membranes, Biochemistry 19 (1980) 3322–3327.

[10] D.M. Tiede, Cytochrome c orientation in electron-transfer complexes with photosynthetic reaction centers of *Rhodobacter sphaeroides* and when bound to the surface of negatively charged membranes: characterization by optical linear dichroism, Biochemistry 26 (1987) 397–410.

[11] D.M. Tiede, P.L. Dutton, Electron transfer between bacterial reaction centers and mobile c-type cytochromes, in: J. Deisenhofer, J.R. Norris (Eds.), The Photosynthetic Reaction Center, Academic Press, San Diego, 1993, pp. 257–288.

[12] Y. Nishimura, S. Mukasa, H. Izuka, K. Shimada, Isolation and characterization of bacteriochlorophyll-protein complexes from an aerobic bacterium, *Pseudomonas radiora*, Arch. Microbiol. 152 (1989) 1–5.

[13] P. Joliot, A. Vermeglio, A. Joliot, Supramolecular membrane assemblies in photosynthesis and respiration, Biochim. Biophys. Acta 1141 (1993) 151–174.

[14] G. Venturoli, A. Mallardi, P. Mathis, Electron transfer from cytochrome c_2 to the primary donor of Rhodobacter sphaeroides reaction centers. A temperature dependent study, Biochemistry 32 (1993) 13245–13253.

[15] R.C. Prince, R.J. Cogdell, A.R. Crofts, The photo-oxidation of horse heart cytochrome c_2 by reaction centers from *Rhodopseudomonas spheroides*, Biochim. Biophys. Acta 347 (1974) 1–13.

[16] D.M. Tiede, A.C. Vashishta, M.R. Gunner, Electron-transfer kinetics and electrostatic properties of the *Rhodobacter sphaeroides* reaction center and soluble c-cytochromes, Biochemistry 32 (1993) 4515–4531.

[17] R.E. Overfield, C.A. Wraight, D. Devault, Microsecond photooxidation kinetics of cytochrome c_2 from *Rhodopseudomonas sphaeroides*: in vivo and solution studies, FEBS Lett. 105 (1979) 137–142.

[18] R. Kort, M.K. Phillips-Jones, D.M.F. van Aalten et al., Sequence, chromophore extraction and 3-D model of the photoactive yellow protein from *Rhodobacter sphaeroides*, Biochim. Biophys. Acta 1385 (1998) 1–6.

[19] T. Leguijt, R.W. Visschers, W. Crielaard, R. Van Grondelle, K.J. Hellingwerf, Low-temperature fluorescence and absorption-spectroscopy of reaction center antenna complexes from *Ectothiorhodospira mobilis*, *Rhodopseudomonas palustris* and *Rhodobacter sphaeroides*, Biochim. Biophys. Acta 1102 (1992) 177–185.

[20] P.L. Dutton, K.M. Petty, H.S. Bonner, S.D. Morse, Cytochrome c2 and reaction center of *Rhodopseudomonas spheroides* membranes. Extinction coefficients, content, half-reduction potentials, kinetics, and electric field alterations, Biochim. Biophys. Acta 387 (1975) 536–556.

[21] R. Clayton, Relations between photochemistry and fluorescence in cells and extracts of photosynthetic bacteria, Photochem. Photobiol. 5 (1966) 807–821.

[22] A. Fersht, Enzyme Structure and Mechanism, W.H. Freeman, New York, 1985.

[23] B.N. Kholodenko, H.V. Westerhoff, Control theory of one enzyme, Biochim. Biophys. Acta 1208 (1994) 294–305.
[24] D.L. Toppen, Letter: kinetics of reduction of horse-heart ferricytochrome c by catechol, J. Am. Chem. Soc. 98 (1976) 4023–4024.
[25] I. Yamazaki, T. Ohnishi, One-electron-transfer reactions in biochemical systems. I. Kinetic analysis of the oxidation-reduction equilibrium between quinol-quinone and ferro-ferricytochrome c, Biochim. Biophys. Acta 112 (1966) 469–481.
[26] A. Labahn, M.L. Paddock, P.H. McPherson, M.Y. Okamura, G. Feher, Direct charge recombination from D^+QaQb^- to DQaQb in bacterial reaction centers from *Rhodobacter sphaeroides*, J. Phys. Chem. 98 (1994) 3417–3423.
[27] D. Kleinfeld, M.Y. Okamura, G. Feher, Electron transfer in reaction centers of *Rhodobacter sphaeroides* I. Determination of the charge recombination pathway of D^+QaQb^- and free energy and kinetic relations between Qa^-Qb and $QaQb^-$, Biochim. Biophys. Acta 766 (1984) 126–140.
[28] D. Kleinfeld, E.C. Abresch, M.Y. Okamura, G. Feher, Damping of oscillations in the semiquinone absorption in reaction centers after successive flashes. Determination of the equilibrium between QA-QB and QAQB-, Biochim. Biophys. Acta 765 (1984) 406–409.